The Mobility of Fractal Aggregates: A Review

C. M. Sorensen
Department of Physics
Kansas State University
Manhattan, KS 66506

Abstract.

A review of the experimental and theoretical literature describing the mobility of fractal aggregates over the previous two decades is presented. Aggregates are those formed via both diffusion and reaction limited cluster-cluster aggregation processes, DLCA and RLCA, which form aggregates with fractal dimensions and prefactors of ca. 1.78 and 1.3 and 2.1 and 0.94, respectively. Emphasis is placed on DLCA aggregates. The entire Knudsen number range from continuum to free molecular is reviewed. The review finds a simple and general consensus description of mobility for the entire range.

1. INTRODUCTION

It is now well established that when solid particles come together via random aggregation processes they form aggregates with fractal morphology. As a consequence, fractal aggregates are ubiquitous in aerosols and colloids in both our natural and technical environments. As such, we desire to know and quantify the physical properties of these particles. Figure 1 shows an electron micrograph of soot fractal aggregates collected from a flame. The particles appear complex, but fortunately we have the quantitative, fractal description of their morphology as a foundation for description of their other physical properties.

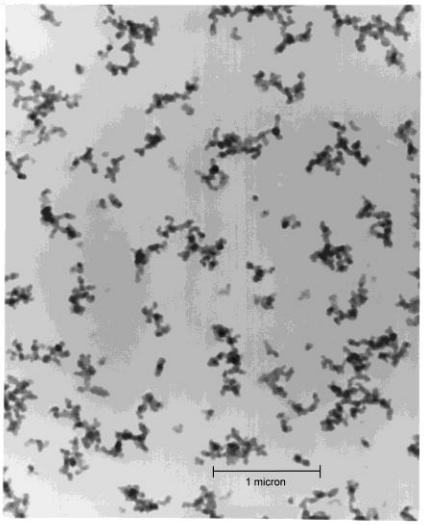

Figure 1. Transmission electron micrograph of soot aggregate particles sampled thermophoretically from an ethene/air laminar, diffusion flame.

This review is concerned with the mobility of fractal aggregates in a medium. Mobility is a fundamental property that determines aggregate transport, dispersal, and the kinetics of their continued growth via aggregation. A considerable body of literature concerning fractal aggregate mobility has developed over the past two and a half decades, but it appears that no review of this literature has been presented. A useful review would critically distill the data and theory to develop a single coherent and hopefully simple description of this phenomenon. It is our purpose here to present such a much needed review.

2. PRELIMINARIES

The mobility of fractal aggregates depends on a number of interweaving factors. There is the fractal nature of the aggregate and the fractal parameters that quantify this nature. There is the size of the aggregate as measured by a linear dimension such as a radius or the number of primary particles or monomers that make up the aggregate. Note that as the size falls to one, the aggregate is no longer fractal. Last but not least is the flow regime which is determined largely by the aggregate's linear size in comparison to the molecular mean free path of the molecules of the medium in which it is moving.

2.1 Fractal Aggregates.

Fractal aggregates are clusters of particles with a self-similar structure over a finite range of length scales. The particles composing the aggregates are called "primary particles" or "monomers". Ideally they are spherical with point contacts, but this description is an approximation. Regardless, we take their radius as *a*, and this sets the lower limit to the fractal scaling range. The upper limit is well described by the radius of gyration R_g which is a root mean square radius that quantifies the overall size of the aggregate. A consequence of self-similarity is that the number of primary particles *N* in the aggregates scales as a power law with the reduced size of the aggregate as

$$N=k_0(R_g/a)^{Df} \tag{1}$$

In Equation (1) D_f is the fractal dimension and k_0 is the scaling prefactor. Equation (1) may be considered as the defining relation for fractal aggregates (see, for example, Sorensen, 2001). A second consequence of scale invariant, self-similarity is that the pair correlation function of the primary particles is a power law which can be expressed as

$$g(r) \sim r^{Df-d}\, h(r/R_g) \tag{2}$$

Here d is the spatial dimension and h(x) is the cutoff function that describes how the aggregate ends at its perimeter. To preserve the power law, h(x) = 1 for x <<1, and to cut off the power law, h(x) must decrease faster than any power law for x >> 1. Such a function that has proven adequate for fractal aggregates is the stretched exponential

$$h(x) = \exp(-x^{\gamma}) \tag{3}$$

Various studies (Mountain and Mulholland, 1988; Cai, Lu and Sorensen, 1995; Lattuada, Wu and Morbidelli, 2003b) have shown $\gamma \sim 2$ to 2.5 for both DLCA and RLCA aggregates (see below).

Aerosol particles almost always aggregate via random Brownian motion; aggregates random walking, meeting and sticking together. Such a process is called Diffusion Limited Cluster Aggregation, DLCA for short (Meakin, 1983; Kolb et al., 1983). In three dimensional space DLCA leads to fractal aggregates with $D_f = 1.78 \pm 0.1$ and $k_0 = 1.3 \pm 0.2$. These numbers can be considered universal since results from a wealth of experiments on both aerosols and colloids (Jullien and Botet, 1987), from simulations (Meakin 1988; Sorensen and Roberts 1997; Lattuada et al. 2003b; Pierce et al. 2006), which show an underappreciated anti-correlation between the fit values of D_f and k_0 (Sorensen and Roberts, 1997), and a simple analytical theory (Sorensen and Oh, 1998) all concur. The prefactor k_0 for some (Koylu and Faeth, 1995), but not

all (Cai et al., 1995), combustion aerosols has been measured to be as large as 2.5, and this possible break from universality appears legitimate and warrants more attention. Moreover, work on some combustion aerosols has suggested D_f = 2.2 to 2.4, but we will demonstrate repeatedly below that this is a result of improper interpretation of mobility measurements. There also are situations where aggregates are found with larger fractal dimensions as a result of processes following the aggregation processes such as shear restructuring or cloud processing. More recently hybrid superaggregates with D_f = 1.8 on short length scales and D_f = 2.6 on larger length scales have been discovered (Sorensen et al. 2003; Kim et al. 2004, 2006). Regardless of these variants, here we will consider the canonical DLCA aggregates which represent the great majority.

In colloids the probability of cluster-cluster sticking upon meeting can be made very small and then a new type of aggregation ensues, Reaction Limited Cluster Aggregation, RLCA. Although RLCA is common in colloids, it seems not to have been observed in aerosols. RLCA leads to D_f = 2.05 to 2.15 with k_0 = 0.94 for the lower D_f value (Lattuada et al., 2003b).

The review below will concern both DLCA and RLCA aggregates with an emphasis on the former.

2.2 The Mobility Radius.

The principle quantitative descriptor of mobility used in this review is the mobility radius. To define the mobility radius we first recognize that the drag force F_d on a particle in a medium moving with velocity v at low Reynolds number can be written as

$$F_d = fv, \tag{4}$$

where f is the drag coefficient. For a spherical particle the drag coefficient is a function of the particle radius, R

$$f = f(R). \tag{5}$$

For a particle of arbitrary shape, we define the mobility radius R_m as that length which yields the correct drag coefficient with the same functionality, f(R), as for a spherical particle

$$f = f(R_m). \tag{6}$$

Many authors use the term “mobility diameter” which is, of course, twice the mobility radius. We shall tend to use “radius” unless referring to work in which diameter values are given.

In this review we will describe the mobility radius in two ways. First, we will compare it to the foremost linear dimension measure of the aggregate size, the radius of gyration, with the ratio

$$\beta = R_m/R_g \tag{7}$$

Second, we will describe its functionality on the foremost mass measure of the aggregate size which is N, the number of primary particles (or monomers), as both

$$N \sim R_m^{Dm} \tag{8}$$

and

$$R_m \sim N^x \quad (9)$$

We call D_m the mass-mobility scaling exponent, and x the mobility-mass scaling exponent. It quickly follows from Equations 8) and (9) that $x = 1/D_m$; hence the reciprocal nature of their names. Although Equations (8) and (9) are redundant, we will find it useful to look at the data both ways.

2.3 The Flow Regime.

The functionality for the drag coefficient depends on the flow regime. The flow regime is determined by the Knudsen number, Kn, which is the ratio of the medium molecule's mean free path to the particle radius (Friedlander, 2000). The definition of the aggregate radius is somewhat problematic; possibilities include R_g, R_m and the mass equivalent radius. Current usage favors R_m , but the exact value is of little consequence for quantification of the mobility radius.

In the continuum regime where Kn <<1 the drag coefficient is given by the Stokes relation

$$f_{St} = 6\pi\eta R_m \quad (10)$$

where η is the shear viscosity of the medium.

In the free molecular regime where Kn >>1, the Epstein equation holds

$$f_{Ep} = 8/3\ \rho\ (2\pi k_B T/m)^{1/2}\ (1 + \alpha\pi/8)\ R_m^{\ 2} \quad (11)$$

where ρ is the medium mass density, k_B is the Boltzmann constant, T the temperature, m the medium molecule mass and α is the accommodation coefficient ($0 < \alpha < 1$, typically $\alpha = 0.91$).

Between these two limits lies the slip or transition regime, where ca. $0.1 < Kn < 10$. Then

$$f = 6\pi\eta R_m/C(Kn) \quad (12)$$

for all Kn where C(Kn) is the Cunningham slip correction factor which is a function of the Knudsen number Kn (Friedlander, 2000).

A simple, general formula good for all Kn is the harmonic sum (Sorensen and Wang, 2000)

$$f^{-1} = f_{St}^{\ -1} + f_{Ep}^{\ -1} \quad (13)$$

This equation has Equations (10) and (11) as limits for small and large R_m, respectively, and is good to 10% or better compared to the standard slip formula, Equation (12), throughout the slip regime. Equation (13) and the slip correction Equation (12) are discussed further in Appendix A.

2.4 Size

Only in the limit $N \rightarrow \infty$ can an aggregate truly be a fractal; all finite sized aggregates are, technically speaking, fractal-like. However, fractal-like aggregates of large N display properties similar enough to their pure fractal ideals to be called "fractal" by those of us with a practical

bent. How large is large enough is an important issue for mobility that we will discuss below. Certainly an aggregate with N = 1, a single sphere, is not fractal, and we will demand that any proper formulation of fractal aggregate mobility must have the correct N = 1 limit. Furthermore, aggregates of two monomers, i.e. doublets with N = 2, have an exact morphology that allows for quantitative description. Hence we will likewise demand that any proper formulation of fractal aggregate mobility must have the correct N = 2 limit as well. An unambiguous shape description is not possible for aggregates with N = 3 or more; for example, if N = 3, the aggregate can be a linear rod or a triangle or some configuration in between these limits.

3. Mobility in the Various Flow Regimes.

3.1 The Continuum Regime.

In the continuum regime the medium is taken as infinitely divisible, hence it has no length scale. Moreover, if the fractal aggregate is asymptotically large, the primary particle size can be neglected relative to the overall size of the aggregate. Thus the only length scale involved in the aggregate mobility problem is the overall size of the aggregate, which is conveniently described by the radius of gyration R_g. Given this, the mobility size, which also has units of length, can only be proportional to the gyration radius. Thus we have

$$R_m = \beta R_g \tag{14}$$

This is a transposition of Equation (7) where β is the ratio of the mobility and gyration radii of the aggregate. A constant ratio β would imply $D_m = D_f$.

Equation (14) holds for "asymptotically" large aggregates. The opposite limit is the single particle aggregate where N = 1. Then the "aggregate" is a single spherical particle with a mobility radius equal to the geometric radius R. For a sphere the radius of gyration is $R_g = \sqrt{3/5}$ R, thus in the single particle limit we must have

$$\beta = \sqrt{5/3} = 1.29. \tag{15}$$

Chan and Dahneke (1981) and Dahneke (1982) first addressed the issue of drag for aggregates with a study of non-fractal, linear chains of spheres. These results have some bearing on the issue for fractals since, as the authors claimed, in the free molecular limit the results should apply to chains with occasional kinks and branches. Also, such chains represent fractal aggregates for N ≈ a few. In particular Dahneke (1982) presented a scheme to calculate the orientationally averaged drag on straight-chain aggregates of all sizes over the entire range of Knudsen numbers. In the continuum limit he did this by extrapolating the data in this limit of Horvath (1974) for straight chains with N = 2, 3, 4, 5 based on analytic expressions for prolate spheroids to arbitrary N. In the free molecular limit he used the Chan and Dahneke results for straight chains. He then developed an interpolation scheme based on the Cunningham correction factor to obtain the drag for arbitrary Kn. Thus all N and all Kn are covered for straight chains.

Figure 2 contains our preliminary and throughout this section evolving picture of the mobility ratio β in the continuum regime. We first plot the orientationally averaged data of Horvath as given by Dahneke. We see that β for the linear chains declines rapidly with increasing N. This is largely due to the rapid increase of R_g with N for the linear chains. Figure 3 plots these same data from the perspective of Equation (9). We find a rough power law with mobility-mass scaling exponent x = 0.52 for N = 1 to 5 and x = 0.56 for N = 1 to 10, the latter

using the Dahneke extrapolation. These values imply D_m = 1.78 to 1.92, similar to the value of D_f for aggregates, not chains. This suggests that naïve use of the mass-mobility scaling relation for linear chains could be miss-interpreted as indication the aggregates have DLCA morphology. Also note that Figure 3 contains both continuum and free molecular results, and we find that the flow regimes are very similar for small N.

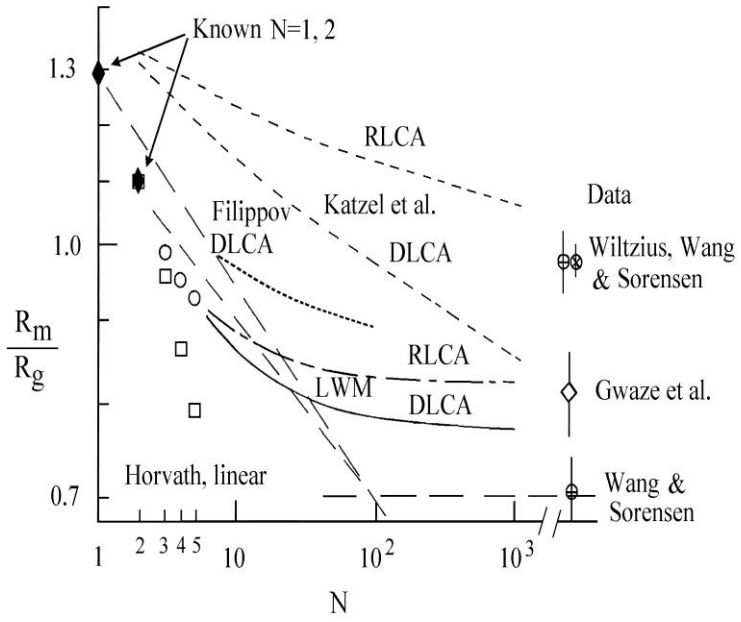

Figure 2. Preliminary graph of the ratio the aggregate mobility radius to the radius of gyration, $\beta = R_m/R_g$, versus the number of monomers (primary particles) in the aggregate N in the continuum limit. Solid diamonds are exact values known for the N = 1 and 2 limits. Data include: open squares are the data of Horvath (1974) for linear chains, circle with X the data of Wiltzius (1987) for RLCA fractal aggregates, circles with plus sign are the data of Wang and Sorensen (1999) for both DLCA and RLCA fractal aggregates, square open diamond the data of Gwaze et al. for DLCA fractal aggregates. Theory includes: solid line Lattuada et al. (2003a), designated by LWM, for DLCA fractal aggregates, dashed dot line Lattuada et al. for RLCA fractal aggregates, short dashed line Filippov (2000), medium dashed line Katzel et al. (2008), and long dashed lines "backbone" functionalities for DLCA fractal aggregates proposed in the text.

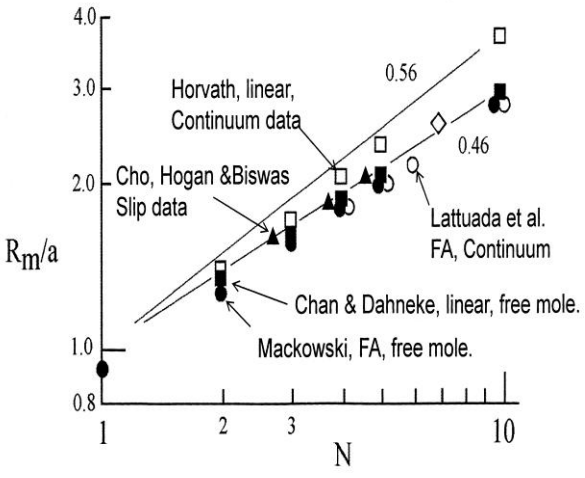

Figure 3. Aggregate mobility radius normalized by the monomer (primary particle) radius, R_m/a, versus number of monomers in the aggregate, N. Open symbols designate continuum regime, closed free molecular regime. Data are open squares from Horvath (1974) for linear chains. Theory includes: closed squares Chan and Dahneke (1981) for linear chains, closed circles Mackowski (2006) for DLCA fractal aggregates, open circles Lattuada et al. (2003a) for DLCA fractal aggregates, and open diamond Binder et al. for a compact seven-star. Lines represent power laws $R_m = aN^x$ for x = 0.46 and 0.56.

Chen, Deutch and Meakin (Meakin, Chen and Deutch, 1985; Chen, Meakin and Deutch, 1987) first addressed the problem of fractal aggregate mobility by application of Kirkwood-Riseman formalism (Kirkwood and Riseman, 1948). This method sums the forces on every primary particle in the aggregate which are due to the interaction of the flow with a given particle plus all the disturbances of the flow due to the other particles. The aggregates they considered were generated via Monte Carlo, cluster-cluster methods to yield both DLCA and RLCA clusters. The primary result of their work was verification of the proportionality expressed in Equation (14). Values of $\beta = 0.875$ and 0.97 were explicitly determined for DLCA and RLCA, respectively, for clusters in the size range N = 50 to 400.

Kirkwood-Riseman theory assumes the spheres that make up the aggregate are widely separated, which is a serious simplification. Despite this caveat, it has the advantage of a straightforward calculation of the coefficient β, *viz.*

$$\beta = \frac{\int_0^\infty r^2 g(r)dr}{\int_0^\infty rg(r)dr} \left[\frac{2\int_0^\infty r^2 g(r)dr}{\int_0^\infty r^4 g(r)dr} \right]^{1/2} . \qquad (16)$$

Figure 4 shows values of β calculated using Equation (16) plotted versus the fractal dimension for a few different correlation function cutoffs (see Equation (3), above). For DLCA with $D_f = 1.78 \pm 0.05$ and $\gamma = 2$ or slightly larger this graph suggests β values of roughly 0.68 to 0.78, the shaded zone on the graph. For RLCA with $D_f = 2.15 \pm 0.05$ and again $\gamma = 2$ or slightly larger this graph suggests β values of roughly 0.83 to 0.91, also shaded in the figure.

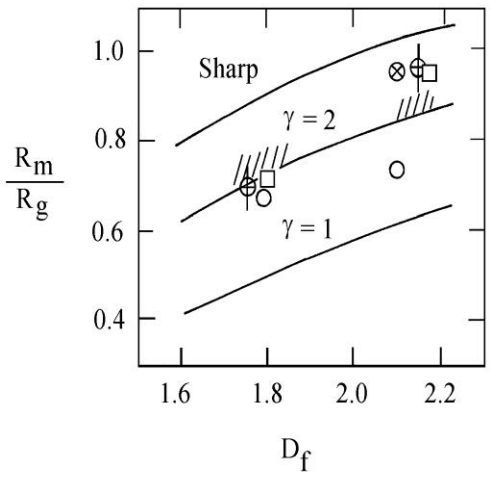

Figure 4. The ratio the fractal aggregate mobility radius to the radius of gyration, $\beta = R_m/R_g$, for large N in the continuum regime versus aggregate fractal dimension, D_f, calculated for three different density correlation function cutoffs using Equation (16). Cross-hatch regions represent reasonable DLCA and RLCA aggregate possibilities. Data included are: circle with X the data of Wiltzius (1987), circles with plus sign are the data of Wang and Sorensen (1999). Other theory includes: open circles, Rogak and Flagan (1990); open squares, Tandon and Rosner (1995).

It appears that Wiltzius (Wiltzius, 1987) was the first to address the problem of fractal aggregate mobility experimentally. He studied a colloidal, RLCA system with $D_f = 2.1$ and used static light scattering to measure R_g and dynamic light scattering to measure R_m. A proper reanalysis of his results (Pusey et al. 1987) to account for the different moments of the size distribution of the aggregates measured by the two different light scattering techniques is needed. Use of this reanalysis with present day knowledge of the RLCA aggregate size distribution (Sorensen and Wang, 1999) yields an experimental value of $\beta = 0.97 \pm 0.02$, in very good

agreement with the Chen, Meakin, Deutch (1987) value. This experimental value is included in Figure 2.

Experimental work from this laboratory (Wang and Sorensen, 1999) included both colloids and aerosols in the continuum regime. Similar to Wiltzius, both static and dynamic light scattering were used to determine the R_g and R_m, respectively. Proper corrections for aggregate polydispersity were carefully made. The colloid was nearly monodisperse Latex microspheres 28 nm in diameter in water destabilized by ionic salt addition. Both the DLCA and RLCA regimes were studied by using different salt concentrations. The measurements yielded fractal dimensions of $D_f = 1.75 \pm 0.10$ and 2.15 ± 0.10, respectively. The aerosol was composed of TiO_2 particles ca. 35 ± 10 nm in diameter. These were allowed to aggregate in air via DLCA at a variety of background pressures from one atmosphere to 1/15 atmosphere to form large aggregates with $D_f = 1.75$. The smallest of these aggregates had $R_g \approx 700$ nm which implies $N \approx 250$.

For the colloid the DLCA yielded values of $\beta = 0.71 \pm 0.05$ and the RLCA yielded $\beta = 0.97 \pm 0.05$. Aerosols for Knudsen numbers in the range $0.02 < Kn < 0.30$ yielded 0.70 ± 0.05. These experimental values are included in Figure 2. The β value increased to 0.75 ± 0.05 when $0.4 < Kn < 1.3$, which is out of the continuum regime.

Wang and Sorensen continued their analysis by considering the theoretical work of others in the continuum regime. Rogak and Flagan (1990) simulated aggregates via an "expanded cube" procedure with selectable fractal dimension. They calculated $\beta = 0.67$ for such clusters when $D_f = 1.79$ and $\beta = 0.73$ when $D_f = 2.1$. Reanalysis of diffusivity calculations by Tandon and Rosner (1995) led to $\beta = 0.71$ and 0.95 for $D_f = 1.8$ and 2.18, respectively. These theoretical values are included in Figure 3.

To summarize the present review to this point, the experimental results are, for the most part, well supported by the various theories. We thus concur (for now) with the 1999 conclusion of Wang and Sorensen that for DLCA with $D_f = 1.75$, $\beta = 0.70 \pm 0.05$, and for RLCA with $D_f = 2.15$, $\beta = 0.97 \pm 0.05$ for asymptotically large fractal aggregates in the continuum regime.

We interrupt our historical review to heuristically develop the small N regime. Values of β for both aggregation mechanisms are less than one, whereas the $N = 1$ limit must have $\beta = 1.29$, Equation (15). Thus the question arises, how does β cross over from the asymptotic values to the $N = 1$ value? A suggestion follows if we relax rigor a bit and think in terms of orders of magnitude. We can argue that one order of magnitude in N is not likely asymptotic, two orders of magnitude to $N \approx 100$ is likely close and three orders of magnitude to $N \approx 1000$ is very probably in the asymptotically large N regime. With this we can propose a functionality for β similar to that sketched in our evolving Figure 2. Here are drawn the "backbone" curves of constant $\beta = 0.7$ at large N and a power law decline from the $N = 1$ value of $\beta = 1.29$ at small N to $\beta = 0.7$ at $N = 100$. "Large" and "small" are separated by $N = 100$. We pick a power law decline in the small N regime merely because fractals often display power law behavior. For DLCA to transform from $\beta = 1.29$ to $\beta = 0.70$ as N varies from $N = 1$ to $N = 100$ requires that

$$\beta = 1.29N^{-0.13} \qquad (17)$$

represent the small N backbone curve (A similar analysis for RLCA yields an exponent of -0.06). Wang and Sorensen proposed a similar crossover for the slip regime based on data from that regime, their figures 7 and 8 where β is plotted versus the Knudsen number. We will discuss this analysis extensively below. The known value for $N = 2$ doublets, 1.09 (Horvath, 1974; Dahneke, 1982: Kasper et al., 1985; Cheng et al., 1988; Kousaka et al., 1996, Zelenyuk et al., 2006) is also

plotted in Figure 2 with the backbone behavior $\beta = 1.18N^{-0.11}$ for the region between N = 2 to 100 (wrong N =1 limit but correct N = 2 limit). Katzel et al. (2008) calculated diffusional behavior for simulated aggregates with tunable fractal dimensions and found behavior qualitatively similar to Equation (17) but the decrease with increasing N continued up to and apparently beyond N = 1000, the largest size studied. However, the small N limit of this work is in error by as much as 20%, see Figure 2. Quite recently Al Zaitone et al. (2009) calculated a dependence well described by Equation (17) for simulated clusters with some sintering in the free molecular regime in the range N = 2 to 200. We now continue with more work involving the continuum regime that mostly vindicates Figure 2.

Filippov (2000) used numerical methods to integrate the interacting Stokesian dynamics of clusters of touching spheres. The aggregates he studied were computer generated and forced to have fractal dimensions of $D_f = 1.0$ (straight chains), 1.2 and 1.8, the latter of which equals that for DLCA. For $D_f = 1.8$ aggregates had prefactors of $k_0 = 1.2$, 1.3 and $k_0 = 2.3$. It is important to point out that whereas these aggregates have D_f and k_0 values the same as or similar to aggregates made via a DLCA process, they might have structural difference from DLCA that in some unknown way affect the mobility. This work involved both continuum and slip flow regimes and was limited to $N \leq 100$. For the DLCA-like aggregates ($D_f = 1.8$) in the continuum regime, β had values of about 0.95, 0.94 and 1.15 for $k_0 = 1.2$, 1.3 and 2.3, respectively, and a very slight decrease of about 3% as N varied from 7 to 100. These results do not support the contention in Figure 2 nor do they agree with the continuum regime measurements of Wang and Sorensen.

Lattuada, Wu and Morbidelli (2003a) extended the Kirkwood-Risemann approach to fractal clusters composed of touching, spherical particles. They derived an analytical expression for the mobility radius for $N \geq 3$ based on the particle-particle pair correlation function, a result analogous to eq. (16). The pair correlation function was determined in a companion paper (Lattuada et al., 2003b) which used a Monte Carlo simulation to create both DLCA and RLCA aggregates. These aggregates had $D_f = 1.85$ and $k_0 = 1.17$ for DLCA and $D_f = 2.05$ and $k_0 = 0.94$ for RLCA. Their results, figure 3 of their paper, are reproduced in our evolving Figure 2 here.

Figure 2 shows that the Lattuada et al. (2003a) results are quite successful in that they support our physical intuition regarding small and large N regimes, the backbone curves in Figure 2, and a crossover between. The asymptotic values at large N are $\beta = 0.765$ and 0.831 for DLCA and RLCA, respectively. This is fairly good agreement with the experiments of Wang and Sorensen for DLCA but not so good for RLCA including Wiltzius's results. Figure 3 shows that the Lattuada et al. calculations for DLCA fractal aggregates fall ca. 15% below the Horvath data for continuum regime linear rods, but are only slightly below the calculations of Chan and Dahneke for free molecular regime linear rods.

Recently Binder et al. (2006) studied the application of Stokesian dynamics methods, exemplified by Filippov's work, and lattice Boltzmann methods for calculating mobility of fractal aggregates in the continuum regime. They considered the lattice Boltzmann method as the most rigorous. It involves a numerical solution to the entire flow field of the aggregate. Their paper compared the two methods for both accuracy and computational efficiency. Aggregates were either doublets, a compact star of seven primary spheres or DLCA simulated with Monte Carlo methods. The doublet result agreed with previous results. The compact, seven membered star result is plotted in Figure 3 and is very consistent with the other linear chain mobilities plotted there. This suggests that the shape is not particularly important in the small N limit. Fractal aggregates with $D_f = 1.85$ of size N = 16, 32, 64 and 128 were describe by $R_m =$

$0.75aN^{0.63}$. This can be converted to β with the aid of eq. (1), their value of and a reasonable guess at $k_0 = 1.17$ to yield $\beta = 0.82N^{0.09}$. This increasing function with N is opposite that expected from the data which led to Figure 2 and the Lattuada et al. result. However, we have replotted their data R_m versus N, log-log and find that the N = 128 point lies off a straight line, power law trend, and its elimination from a fit to Equation (9) implies $R_m = aN^{0.55}$, consistent with the implication that β is constant in this regime.

We now summarize mobility for the continuum regime. This summary uses the judgment of the author to select results that are consistent with each other. A combination of theory and experiment (see also the discussion of Gwaze et al. (2006) who found an experimental value of $\beta = 0.81 \pm 0.07$, below) suggests that asymptotically large DLCA fractal aggregates have a constant ratio $\beta = 0.75 \pm 0.05$. Asymptotically large RLCA aggregates have $\beta = 0.97 \pm 0.05$. Moreover there appears to be a crossover in functionality near $N \approx 100$. Backbone functionalities for DLCA aggregates in the small and large N regimes are

$$R_m = aN^{0.46}, \qquad N < 100 \tag{18a}$$

$$R_m = 0.65aN^{0.56}, \qquad N > 100 \tag{18b}$$

Equation (18a) has the correct N = 1 and 2 limits; Equation (18b) yields $\beta = 0.75$ for fractal aggregates with $D_f = 1.78$ and $k_0 = 1.3$. Equations (18a) and (18b) crossover at N = 74 (This is not significantly different than 100 because the result depends sensitively on the difference in the exponents 0.56 - 0.46 = 0.10).

3.2 The Free Molecular Regime.

Since aggregates have two length scales, overall aggregate and primary particle sizes, the concepts of Knudsen number, which compares the particle size to the medium molecule mean free path, and the concomitant free molecular regime, can be ambiguous. In this work we shall use "free molecular" to mean that the mean free path is large compared to the overall aggregate size. This is consistent with the use of the mobility radius for defining the Knudsen number of an aggregate as stated above.

The physics of the free molecular regime drag is straightforward enough to allow for reasonable physical, although not rigorous, arguments for the functionality of mobility radius on the number of primary particles in the aggregate. The physics is simply that the medium is not a medium at all but rather a collection of widely separated molecules traveling ballistically in straight lines that impart drag to any object by colliding with it. The probability of collision is proportional to the available geometric cross section of the object. This available geometric cross section is the projected area of the aggregate perpendicular to a molecule's linear path due to the relative velocity between the molecule and the aggregate averaged over all directions in space that the molecules may take. Thus the drag on a sphere is proportional to the square of the geometric radius, a^2, and the drag on an aggregate of N spherical particles of radius *a* is proportional to Na^2. Then the mobility radius is $R_m = aN^{0.5}$.This zeroth order result needs modification due to primary particle-particle screening or shadowing of the ballistic molecules. This would tend to make the functionality of the cluster projected area on N less than linear. These projected area arguments lead to a mobility radius given by

$$R_m = aN^x \quad (19)$$

where the exponent $x < 0.5$ is, as first defined in Equation (9), the mobility-mass exponent. Note that Equation (19) has the correct $N = 1$ limit. As an example note that a dense aggregate with $D_f = 3$ would have $x = 1/3$. From this it is tempting to propose that for a fractal aggregate of arbitrary D_f, $x = 1/D_f$. This, however, will prove not to be true. The question is, what is x?

Meakin, Donn and Mulholland (1989) created simulated aggregates with $D_f = 1.8$ and determined their projected area as a function of N. They found that the projected area of the cluster, A_c, ratioed by the projected area of the primary particle, A_p, could be fit empirically to

$$A_c/A_p = 0.4784N + 0.5218N^{0.7697} \quad (20)$$

The square root of this, which is proportional to the mobility radius, can be fit to the power law of Equation (9) with $x = 0.455$ for $N = 1$ to 100, $x = 0.461$ for $N = 1$ to 1000 and $x = 0.462$ for $N = 10$ to 1000.

Pierce, Chakrabarti and Sorensen (2006) studied the projected area of cluster-cluster aggregates formed from diffusive motion in the continuum with Stokes drag, diffusive motion in the free molecular regime with Epstein drag and cluster ballistic motion in the extreme free molecular regime. Aggregate sizes ranged from $N = 10$ to 300 and the fractal dimension for the Epstein regime aggregates was 1.80 to 1.82, depending on the method of analysis, with $k_0 = 1.24$. Aggregates formed via all schemes led to essentially the same mass-mobility exponent of $x = 0.46 \pm 0.002$.

Recently, Al Zaitone, Schmid and Peukert (2009) simulated aggregates with various degrees of sintering. Aggregate sizes ranged from $N = 2$ to 200. The free molecular mass-mobility exponent that can be inferred from their work is $x = 0.46$.

The first rigorous calculation of drag on an aggregate was done by Chan and Dahneke (1981) who considered linear chains of touching spherical particles in the free molecular regime. Their method was a Monte Carlo technique that determined the rate of momentum transfer, hence the drag force, due to molecular collisions with the aggregate. As mentioned above, they claimed that their results applied to chains with occasional kinks and branches so long as these perturbations on linearity did not introduce significant additional monomer-monomer screening effects. The result can be expressed as a mobility radius of the form

$$R_m = a\sqrt{0.802(N-1) + 1} \quad (21)$$

Results from Equation (21) are plotted in Figure 3 for the range $N = 1$ to 10. The approximate linearity of the results on this log-log plot implies that this formula can be recast very well in the form of the power law of Equation (9). We find the mobility-mass exponent $x = 0.446$ for the range $N = 1$ to 5 and 0.458 for the range $N = 1$ to 10. Thus the exact numerical calculations of Chan and Dahneke are very consistent with the projected area concepts above. Moreover, they lead to essentially the same mobility-mass exponent.

Mackowski (2006) has presented an important paper which calculates the drag on fractal aggregates of spherical particles in the free molecular regime. His method followed the Monte Carlo approach of Chan and Dahneke to simulate the exchange of momentum and energy between the colliding molecules and the particles that make up the aggregate. Unlike that work,

however, a slow moving flow condition was used which improved the accuracy and convergence of the method. The aggregates used were created via a sequential algorithm to produce synthetic cluster-cluster aggregates with predetermined D_f and k_0 in the ranges 1.7 to 2.0 and 0.7 to 2.0, respectively. His empirical fit to all his numerical results for N = 2 to 3000 is

$$R_m = 1.624a k_0^{-1/Df} D_f^{-0.9} N^{0.47} \qquad (22)$$

These very general results yield a mobility-mass exponent of x = 0.47, quite consistent with all the results above. Results from Equation (22) are also plotted in Figure 3 for $D_f = 1.78$ and $k_0 = 1.3$. There it is seen that the Mackowski results are shifted down about 8% relative to Chan and Dahneke and the trend of Equation (19) with x = 0.46 because the prefactor of Equation (22) is 0.915 for these values of D_f and k_0.

Data for aggregate mobility deep in the free molecular regime are difficult to obtain because the mean free path in N_2 at STP is 66 nm and primary particles typically have radii of 15 nm or larger. Once an aggregate forms from these particles, the aggregate size is comparable to the mean fee path and hence in the slip regime. Wang and Sorensen (1999) tried using pressures down to 1/15 atmosphere where the mean free path is 990 nm but still the largest Knudsen number they achieve was 1.3.

It appears that the data set with the largest Knudsen numbers are those obtained by Cai and Sorensen (1994) who studied soot fractal aggregates in flames. Their flame environments were at atmospheric pressure but at elevated temperatures such that the mean free paths were ca. 330 nm to yield Kn in the range 4 to 16. Their method was the same as Wiltzius (1987), DLS was used to measure R_m and SLS was used to measure R_g. Proper analysis was used to deconvolute the effects of aggregate polydisperity. Scattering extinction measurements were performed to measure optically N and a (Sorensen, Cai and Lu, 1992). The soot was fractal with $D_f = 1.79 \pm 0.1$ and N in the range 4 to 35. They found the ratio β was not constant but instead $\beta \sim N^{-0.13}$. The exact dependence found is

$$R_m = 0.99aN^{0.43} \qquad (23)$$

with the error of 0.99 ± 0.08 and $x = 0.43 \pm 0.03$. This result has both the correct N = 1 limit and very good agreement for the mobility-mass exponent with the theories above.

Cai and Sorensen interpreted their result as indicative of the importance of the projected area seen by the ballistic molecules of the medium for the effective drag and cited corroboration with Meakin, Donn and Mulholland (1989), discussed above. They also likened the screening of ballistic molecules to the screening of electrons during TEM observation of fractal aggregates. TEM analysis finds that the projected area of the aggregate in the electron beam is sublinear with N, *viz.* $\sim N^{0.9}$, which is consistent with a mobility-mass exponent of 0.45.

As for the continuum regime, we now form a summary that uses the judgment of the author to select results that are consistent with each other. We find that the aggregate mobility in the free molecular regime is well described by mass-mobility and mobility-mass exponents of $D_m = 2.17 \pm 0.10$ and $x = 0.46 \pm 0.02$, respectively, for DLCA aggregates of all sizes N. We therefore write

$$R_m = aN^{0.46} \qquad \text{for all N.} \qquad (24)$$

Equation (24) has both the correct N = 1 and 2 limits. Now note the remarkable similarity between Equations (18a) and (24). We find that the mobility behavior in the continuum and free molecular flow regimes is, within a small uncertainty, the same in the small N regime. This appears to be a coincidence because the physics of mobility is different in the two flow regimes.

3.3 The Slip Regime

There have been numerous measurements of fractal aggregate mobility in the slip regime published in the aerosol literature. Many of these studies have found a power law relationship between the mobility radius and the number of primary particles in the aggregate in the form of the standard "fractal" equation, Equation (8) reproduced below

$$N \sim R_m^{Dm} \tag{8}$$

and have called the exponent D_m the fractal dimension. Some workers have noted that D_m determined via Equation (8) does not equal the fractal dimension determined via other methods. We will show below that interpretation of D_m in Equation (8) as the fractal dimension is erroneous, misled by a subtle combination of the behavior of mobility in the slip regime and the small N limit.

Before we address the mobility aspects of Equation (8), it is important to recall the meaning of the fractal dimension in the defining relation, Equation (1). The fractal dimension quantifies the power law scaling of the mass of the aggregate, which is proportional to N, with a measure of its linear size. The radius of gyration, depending only on the spatial arrangement of the mass in the aggregate and nothing else, is an intrinsic quantity, hence it is a proper measurement of the linear size of the aggregate. The mobility radius, on the other hand, depends not only on the arrangement of the mass in the aggregate but also on features in its environment not intrinsic to the aggregate such as flow regime and aggregate alignment relative to the flow, and therefore is not a proper measure of linear size. Consequently, mobility radius should not be used to determine the fractal dimension without knowledge of how it is related to a true measure of linear size, such as the radius of gyration.

Measurements of mobility of aerosol fractal aggregates were pioneered by Schmidt-Ott (1988) who evaporated silver to create primary particles with a radius of 7.5 nm. These were allowed to aggregate, presumably via DLCA, and then their mobility size was measured with a Diffusion Mobility Analyzer (DMA). After passing out of the DMA, the aggregates were sintered at elevated temperature to form compact aggregates which then passed through a second DMA to obtain the compact aggregate mobility size which is the geometric radius and directly related to the mass via a cubic scaling law. Both DMA's operated at ambient. From these two measurements a mass-mobility description of the aggregates was obtained and fit to Equation (8) to yield $D_m = 2.18$. This was interpreted as the fractal dimension D_f of the aggregate.

Wang and Sorensen (1999) reanalyzed Schmidt-Ott's data assuming the aggregates were truly the result of DLCA and therefore had a fractal dimension of $D_f = 1.75$, not 2.18. Their conclusion was that the aggregates were in the small N regime where, as we have seen above for the continuum and free molecular regimes, R_m and R_g are not proportional. Then D_f of Equation (1) will not equal D_m of Equation (8). Figure 3 of Schmidt-Ott and the primary particle radius can be used to infer the number of primary particles in the clusters. The values range from $N \approx 2$ to 37. This is well within the small N regime for the continuum flow, Figure 2 above, with the backbone behavior of Equation (17). If we take $D_f = 1.75$, then $R_g \sim N^{0.57}$. Application of this

with Equations (7) and (17) yields $R_m \sim N^{0.44}$. This implies for the mass-mobility relation, Equation (8), $D_m = 2.26$, consistent with Schmidt-Ott's value. Reasoning in reverse, the Schmidt-Ott value $D_m = 2.18$ coupled with $D_f = 1.75$ imply the exponent in Equation (17) should be -0.11, the value obtained using the N = 2 limit, very reasonable for the physical argument given there.

Wang and Sorensen also reanalyzed the data of Rogak, Flagan and Nguyen (1993). These workers used a tandem DMA, pre- and post-sintering method ala Schmidt-Ott with both TiO_2 and SiO_2 aerosols. By assuming these aggregates were the result of DLCA hence have $D_f = 1.75$, they showed that the exponent in Equation (17) would be -0.12 and $D_m = 2.22$.

Since 1999 there has been a plethora of measurements of aerosol fractal aggregate mobility all of which have been in the slip regime, typically with Kn < 1. Moreover, nearly all have involved aggregates that could be classified as small by our evolving point of view. We now review all these works with an eye towards a consistent interpretation involving both the proposition that all these aggregates are the result of DLCA, hence have a D_f of about 1.78, and that at least part of any given study involved aggregates in the small N regime. This latter point is particularly important for we have seen that the mobility behavior in the continuum and free molecular flow regimes is nearly the same for small N. Thus we expect that the slip flow regime, which resides between these two, will have the same behavior as well and that behavior is described by a mass-mobility exponent of $D_m \approx 2.2$.

Cho, Hogan and Biswas (2007) purposely studied aggregates with a small number of primary particles in the transition regime. Their method used nearly monodisperse polystyrene latex spheres with diameters of 55, 67, 76, 99 nm obtained by spray drying colloids of these spheres. The method was essentially that of Schmidt-Ott. The mobility diameter of aggregates of N=3, 4 and 5 of these primaries was measured with a DMA and then these were sintered in a furnace to create spheres. The mobility diameter of these sintered spheres was measured by a second DMA. The sintered sphere mobility diameter agreed very well with the diameter that can be calculated based on conservation of mass, the mass equivalent diameter. All the mobility diameters ranged from ca. 80 to 200 nm, hence given an ambient condition's air mean free path of 66nm the flow is in the transition regime with Kn = 0.66 to 1.65.

Cho et al. fit their results to a three parameter power law of the form of Equation (9) which found a mobility exponent of x = 0.426. This fit also found a slightly nonlinear dependence on primary particle diameter and had a bad N=1 limit. We have refit the data to the simple Equation (9) including the N=1 point as well. We find x= 0.44.

Park, Kittleson and McMurry (2004) studied diesel exhaust particles. Using TEM they compared aggregate length to projected area which can be related to total mass. This analysis yielded fractal dimensions of $D_f = 1.61$ and 1.75, depending on the details of the analysis. These values are consistent with DLCA. Using DMA and APS they obtained aggregate mass as a function of mobility diameter over the range 50 to 300 nm. This yielded a mass-mobility scaling exponent of $D_m = 2.35$. The primary particle mean diameter was 32 nm. We can use these values, assume $R_m = 0.7R_g$, $k_0 = 1.3$ and Equation (1) to estimate, very roughly, the N value in this size range to be ca. 5 to 110. This is within the small N regime as we have described above and hence can explain the large mobility-mass scaling exponent compared to the fractal dimension. $D_m = 2.35$ can be inverted to yield a mobility-mass exponent of x = 0.426.

Maricq and Xu (2004) used a tandem DMA and an electrical low pressure impactor to compare aggregate effective density to mobility diameter for both premixed ethylene flames and diesel exhaust soot. In their review of the literature they point out the inconsistency of fractal dimensions measured via mobility analysis that tend to be larger than those measured via TEM

analysis, exactly the problem addressed here. Ethylene flames yielded soot mobility diameters in the range 36 to 200 nm with an effective primary particle diameter of 16 to 26 nm depending on the height above the burner from which the soot was sampled. Measured density versus mobility diameter yielded mass-mobility scaling exponents of D_m = 2.1 to 2.2. Diesel exhaust yielded soot mobility diameters in the range 30 to 320 nm with an effective primary particle diameter of 16 to 25 nm. Density versus mobility diameter yielded D_m = 2.2 to 2.35. We can use these values, a fractal dimension of 1.78, a prefactor of $k_0 = 1.3$, $\beta = 0.7$ and Equation (1) to estimate the N values to be in the range ca. 4 to 350. That's over a decade within and half a decade out of the small N regime. According to the argument being presented here, the former smaller decade of size would see a scaling exponent of ca. 2.2; the latter half decade would see a scaling exponent of ca. 1.8. Close inspection of their figures plotting effective density versus mobility diameter shows that the slope of these double logarithmic plots is increasing with increasing mobility diameter. Since the slope is D-3 this implies D is decreasing with increasing mobility diameter, as we predict. If we regard the mass-mobility scaling exponents obtained by Maricq and Xu as showing the functionality of mobility in the small N limit as portrayed in Equation 8, then we obtain the mobility-mass exponent in the range x = 0.425 to 0.476.

De Carlo et al. (2004) and Slowik et al. (2004) presented back-to-back papers with an extensive review and study of the effects of particle morphology on density characterization and mobility. Following Wang and Sorensen (1999) and Baron, Sorensen and Brockman (2001), they concurred that the mass-mobility scaling had two regimes depending on size and concluded that the crossover was at N=60. However, they erroneously use the term "fractal dimension" to describe the power law scaling in each regime claiming that there are two distinct values of the fractal dimension and that it transitions smoothly between the two regimes. These conclusions are simply fixed by replacing "fractal dimension" by "mass-mobility scaling exponent". Slowik et al. present data on soot extracted from a premixed propane "air" flame with mobility measured by a DMA and mass by an aerosol mass spectrometer.

Van Gulijk et al. (2004) confronted the reinterpretation of the Schmidt-Ott (1988) data by Wang and Sorensen (1999) by casting nebulous dispersions on the light scattering technique. This author could spend some time here demonstrating the reliability of light scattering for fractal aggregate measurements. Instead, we point out that Van Gulijk et al. failed to realize that Wang and Sorensen used the data of Schmidt-Ott (1988) and of Rogak, Flagan and Nguyen (1993), neither of which used light scattering, to help uncover the problem that there is a small N limit in which the caution we are trying to convey exists. The different functionalities of the mobility radius depending on size exist in non-light scattering data.

The experiments of Van Gulijk et al. studied soot from a diesel engine. A scanning mobility particle sizer measured the mobility diameter of the aggregates and an electrical low-pressure impactor measured the aerodynamic diameter. The data were obtained in the transition slip flow regime. The relationship between these diameters in the transition regime yielded a "fractal dimension", based on the mass-mobility scaling relation, of 2.4. As we have seen, this is pretty typical for D_m in the small N regime. The primary particle diameters were 35 nm; the mobility diameters were in the range 75 to 280 nm. From this we can estimate, as described above, $N \approx 10$ to 100, values that are within the small N regime. Very interesting is that even casual examination of the analysis presented in their figure 4, shows that the log-log plot of the five data points is not linear as expected for the simple power law expression for the analysis, their equation 24, which yielded "fractal dimension" of 2.4. In fact, the first two points have a stronger slope to imply a "fractal dimension" approaching 3, a reasonable value for an aggregate

of only a few or less primary particles. Most interestingly, the last two points at the largest size have a slope of nearly zero, which by their equation 24 would imply a "fractal dimension" of 1.8. This is exactly what we expect as the mass-mobility scaling exponent becomes equal to the true fractal dimension as the aggregate size grows out of the small N limit! The data of Van Gulijk et al. support our argument.

Gwaze et al. (2006) studied fractal aggregates created from wood combustion under flaming conditions. The soot was size classified using a DMA to obtain aggregates with mobility radii of 100 to 396 nm. Subsequently these aggregates were collected via impaction on filter membranes for SEM analysis which yielded monomer size of 25.5 nm and fractal analysis that gave an average fractal dimension of $D_f = 1.83$. The scaling of the mobility radius with N had a mobility-mass exponent of $x = 0.56 \pm 0.04$ which is equivalent to a mass-mobility scaling exponent of 1.79 consistent with the measured D_f. The measured number of primary particles for the range of mobility sizes studied ranged from ca. 23 to 420. Since some of this range is in the small N regime, it is somewhat surprising that the mobility scaling exponent compares so well to the fractal dimension. On the other hand a considerable part of the range is in the large N regime where the two exponents are equal. The aggregate R_g was also measured from the SEM images. This combined with the mobility led to a value of $\beta = 0.81 \pm 0.07$ for the Knudsen range 0.17 to 0.5.

Very recently Shin et al. (2009, 2010) presented careful studies of the friction coefficient of silver aggregates in the transition regime. The methods involved using a DMA to select a mobility size and then an Aerosol Particle Mass analyzer (APM) to measure the aggregate mass or a tandem DMA to measure mobility before and after aggregates sintering to spherical particles. The carrier gas was N_2 at ambient. Primary particle sizes in the first study were 16 and 20 nm diameters for two different runs. Aggregate mass and primary particle size lead to primary particle number, which were in the range N = 40 to 600. In both studies TEM showed highly neck structures and analysis yielded fractal dimensions in the range $D_f = 1.74$ to 1.84, although there is some question whether these values should be scaled up by ca. 10% due to errors in interpreting 2d projections of the 3d aggregates. In the first study a mass-mobility comparison yielded an exponent of $D_m = 2.10 \pm 0.065$ for mobility diameters ranging from 37 to 300 nm, hence Kn in the range 0.44 to 3.6. In the second study values of $Dm = 2.172 \pm 0.036$ and 2.126 ± 0.061 were found for the DMA-APM and TDMA, respectively. All these values are consistant with the results discussed above.

In summary, in the slip, small N regime, the mass-mobility and mobility-mass exponents are well described by $D_m = 2.22 \pm 0.1$ and $x = 0.45 \pm 0.02$, respectively. These exponents are essentially equal to those found in both the continuum and free molecular regime. Interpretations that claim the fractal dimension equals the mobility-mass scaling exponent, i.e. that $D_f = D_m$, for small N slip are wrong. Whereas the literature offers examples of slip regime data that transform into the continuum regime at large N, there appear to be no large N, slip regime data.

4. Overall Summary and Conclusions.

We now pull together and summarize all the results above, both experimental and theoretical, and make thoughtful conclusions for a best, general description of fractal aggregate mobility to date across the entire range of Knudsen numbers. It is important to stress that what follows is the author's best attempt for a distillation of the review above regarding functionality, numerical values and error estimates for those values.

The general description for the mobility of DLCA fractal aggregates quantified by D_f = 1.78 and k_0 = 1.3 in the limits of Kn → 0 and Kn → ∞ is given by back bone Equations (18) and (24), respectively, which we reproduce here:

Continuum Regime, Kn → 0, $R_m = aN^{0.46}$, $N < 100$ (18a)

$R_m = 0.65aN^{0.56}$, $N > 100$ (18b)

Free Molecular Regime, Kn → ∞, $R_m = aN^{0.46}$ for all N. (24)

The error in the exponents is estimated to be ± 0.02. These results are displayed in Figure 5.

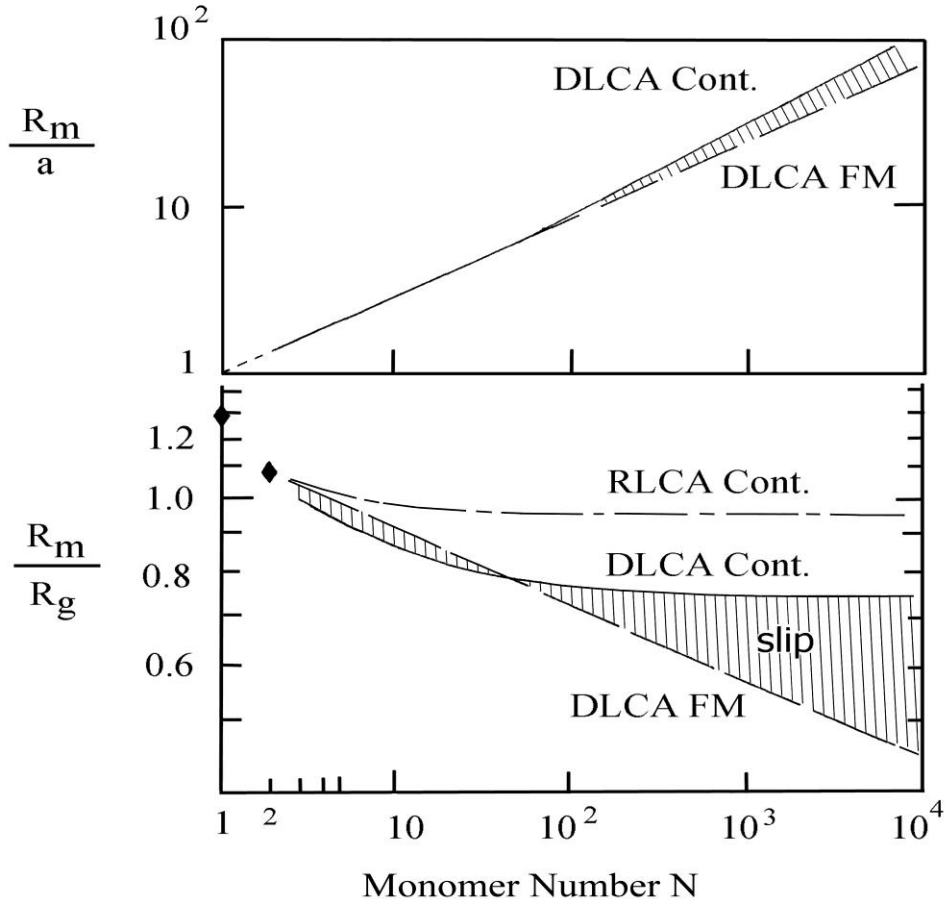

Figure 5. General description of the mobility of fractal aggregates. Lower half shows the ratio of the aggregate mobility radius to the radius of gyration, $\beta = R_m/R_g$, versus the number of monomers (primary particles) in the aggregate, N. Filled narrow diamonds are exact results for N = 1 and 2. Solid line is for DLCA fractal aggregates in the continuum regime, long-short dashed line is for RLCA fractal aggregates in the continuum regime, long dashed line is for DLCA fractal aggregates in the free molecular regime. Upper half shows the ratio of the aggregate mobility radius to the monomer (primary particle) radius, R_m/a, versus the number of monomers in the aggregate, N. Solid line is for DLCA fractal aggregates in the continuum regime, long dashed line is for DLCA fractal aggregates in the free molecular regime. The lines overlap on this scale for N < 100.

The lower half of Figure 5 shows a plot of the ratio of the mobility radius to the radius of gyration, $\beta = R_m/R_g$, versus the number of monomers (primary particles) in the aggregate, N, in both the continuum and free molecular regimes. This is a remake of and a replacement for our preliminary graph in Figure 2, based on our assessment of Figure 2. In Figure 5 we see that in the continuum regime the ratio β falls from known values at N = 1 and 2 to asymptotic values of 0.75 ± 0.05 and 0.97 ± 0.05, for DLCA and RLCA, respectively, as N goes to infinity. The small N (where β varies) to large N (where β is constant) regimes crossover near N ≈ 100. The free molecular regime result is shown only for DLCA aggregates. It is represented by Equation (24) ratioed by the solution of Equation (1) solved for R_g using $k_0 = 1.3$ and $D_f = 1.78$. Such a solution yields the correct value for R_g for N = 2, but not for N = 1. Thus the long dashed line representing this result limits to the correct N = 2 value.

The upper half of Figure 5 shows the mobility radius ratioed to the primary particle radius, R_m/a, versus the number of monomers (primary particles) in the aggregate, N, for DLCA aggregates only. Slopes on this log-log graph are the mobility-mass exponent x. In the continuum regime for small N (N < 100) this graph displays the approximate power law where the mass-mobility exponent is x = 0.46 ± 0.02, Equation (18a). We stress that the exact functionality in this range of N is not exactly the backbone power law but rather the curving asymptotic approach similar to that calculated by Lattuada et al. (2003) and drawn for β in the lower half. However, experiment has shown that this curvature is hard to discern, the data are often well described by the power law, and the power law is very close to the curve. For large N (N > 100) the functionality crosses over to Equation (18b) with an exponent equal to the inverse of the fractal dimension.

The upper half of Figure 5 also shows R_m/a versus N in the free molecular for DLCA aggregates. Remarkably the behavior is essentially the same as the continuum regime behavior for small N.

We remark that for DLCA aggregates in the free molecular regime the results here imply $\beta \sim N^{-0.1}$. Thus β goes to 0 as N goes to ∞. This somewhat surprising result is a consequence of the decreasing density as the aggregate gets bigger. However, it does call into question the use of the mobility radius for defining the Knudsen number, an issue which will not be addressed here.

The slip regime lies between these two limits. With the help of either the lower or upper halves of Figure 5, it is not too difficult to picture what the functionalities of β or R_m/a are as Kn evolves from 0 to ∞. In the lower half plot, the continuum limit at N > 100 would rotate downward with increasing Kn until it met the continuum limit drawn there, while for 2 < N < 100 the continuum curve would flatten slightly upward to meet the free molecular line. The picture is even simpler in the upper half, where for N > 100 the continuum limit straight line with slope 0.56 would rotate downward about the N = 100 point until it met the free molecular line with slope 0.46 with increasing Kn; there would be essentially no visible change for N < 100. These simple transformations describe the entire slip transition regime, i.e. the slip regime lies in the small regions between the continuum and free molecular plots in Figure 5.

This graphical picture of what happens in the slip regime for N > 100 can be expressed by an empirical formula

$$R_m = a(10^{-2x + 0.92})\, N^x \quad , \qquad \text{where } 0.46 < x < 0.56. \qquad (25)$$

In Equation (25) the mobility-mass scaling exponent x is now a function of the Knudsen number. Note that Equation (25) has the proper limits at x = 0.46 and 0.56. Since the slip regime roughly spans 0.1 < Kn < 10, the extremes of which have x = 0.56 and 0.46, respectively, we can propose that x varies geometrically across that range. Thus for example, if Kn = 1, x = 0.51, if Kn = 3, x = 0.485, etc. It is hoped that someday data will be obtained in this regime to test this proposal.

The dynamic shape factor of a particle can be defined as the ratio of the drag force on the particle divided by the drag force on the particle's volume equivalent sphere (Baron et al.2001). Thus

$$\chi = f(R_m)/f(R_{ve}) \tag{26}$$

where $R_{ve} = aN^{0.33}$ is the volume equivalent sphere radius. With Equation (12) this becomes

$$\chi = R_m C(Kn_{ve})/R_{ve} C(Kn_m) \tag{27}$$

where Kn_{ve} and Kn_m are the Knudsen numbers using the mobility radius and the volume equivalent radius, respectively.

With Equation (27), the dynamic shape factor can be calculated for a DLCA fractal aggregate with N < 100 using $R_m = aN^{0.46}$ (Equations (18a) and (24)) and for N > 100 using Equation (25). The results for a variety of mobility radius Knudsen numbers using the constant A = 1.612 (see Appendix A) are given in Figure 6. The nonmonotonic behavior with Kn_m for N > 1000 is due to the fact that at large N the ratio R_m/R_{ve} becomes so large that the quadratic functionality of the drag with linear size dominates even at small Kn_m.

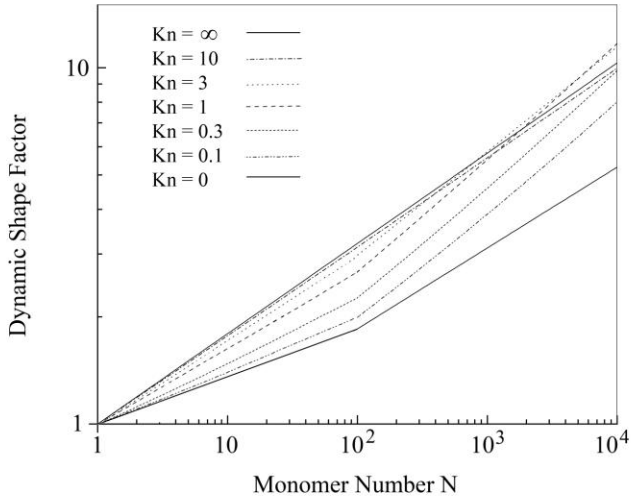

Figure 6. Dynamic Shape Factor of DLCA fractal aggregates for a variety of mobility radius Knudsen numbers as a function of the number of primary particles (monomers) in the aggregate.

To conclude, we return to Figure 5 which presents a distillation of the experimental and theoretical work on the mobility of fractal aggregates to date. It is an elegantly simple and comprehensive summary of how the fractal aggregate mobility is related to mass N and size R_g.

Appendix A.

Here we illustrate the usefulness of the harmonic sum, Equation (13), above, and reproduced here

$$f^{-1} = f_{St}^{-1} + f_{Ep}^{-1} \tag{13}$$

as a general formula for the friction coefficient. The microscopic and macroscopic domains of a fluid are connected by the formula

$$\eta/\rho = \varphi u \lambda \tag{A1}$$

The macroscopic quantities are η the shear viscosity and ρ the mass density of the fluid medium; the microscopic quantities are the mean thermal molecular velocity $u = (8kT/\pi m)^{1/2}$, where k_B is Boltzmann's constant, T the temperature, and m the medium molecular mass; and λ the medium molecule mean free path. The constant $\varphi = 0.499$ for elastic, hard sphere molecules. With this, the Epstein drag coefficient, Equation (11), can be written

$$f_{Ep} = (4\pi/3)\eta\, R_m^{\,2}\, [(1 + \alpha\pi/8)/\varphi\lambda] \tag{A2}$$

Substitution of this along with the Stokes formula, Equation (10), into the harmonic sum formula with some minor algebra yields

$$f = 6\pi\eta R_m/(1 + A\lambda/R_m) = 6\pi\eta R_m/(1 + A\ Kn) \tag{A3}$$

where $Kn = \lambda/R_m$ is the Knudsen number and $A = 9\varphi/2(1 + \alpha\pi/8)$. The constant can be evaluated for $\alpha = 1$, a reasonable value, as $A = 1.612$.

With a constant $A = 1.612$, Sorensen and Wang (2000) demonstrated that the predicted value of the drag coefficient is accurate at the limits $Kn = 0$ and $Kn >> 1$, and is in error by as much as 10% too small near $Kn = 0.5$ relative to the standard Cunningham correction. The Cunningham correction would replace the constant A in Equation (A3) with

$$A(Kn) = \alpha + \beta \exp(-\gamma/Kn) \tag{A4}$$

The constants α, β and γ are determined empirically by fitting to Millikan's data. Allen and Raabe (1982) give $\alpha = 1.155$, $\beta = 0.471$ and $\gamma = 0.596$. However, the random error in the Millikan data are about 5%, which is half the discrepancy incurred by using the constant A. Moreover, as pointed out by Sorensen and Wang (2000), the 10 % error is comparable to other uncertainties endemic in aerosol transport and kinetics studies. Hence use of Equation (A4) barely warrants the additional complexity.

Acknowledgements. My work in this area has benefited from the pleasant and stimulating collaboration with my students J. Cai, N. Lu, G. M. Wang, C. Oh, R. Dhaubhabel, D. Fry, F. Pierce and colleague Amit Chakrabarti. This work has benefited from communications with G. Mulholland, W-G. Shin, S. Rogak, A. Filippov, J. Slowik, P. Gwaze, W. Peukert. My work has been supported by the NSF and NASA.

References.

Allen, M. D., and Raabe, O. G. (1982). Re-Evaluation of Millikan's Oil Drop Data for the Motion of Small Particles in Air, *J. Aerosol Sci.* 13:537-547.

Al Zaitine, B., Schmid, H.-J., and Peukert, W., (2009). *J. Aerosol Sci.* 40:950-964.

Baron, P., Sorensen, C. M., Brockman, J. (2001). Nonspherical Particle Measurements: Shape Factors, Fractals and Fibers, in Aerosol Measurement, ed. by P. Baron and K. Willeke, Wiley-Interscience, New York.

Binder, C., Hartig, M. A. J. and Peukert, W. (2009). Structural dependent drag force and orientation prediction for small fractal aggregates, *J. Coll. Int. Sci.* 331: 243-250.

Binder, C., Feichtinger, C., Schmid, H.J. and Thürey, N. (2006). Simulation of the Hydrodynamic Drag of Aggregated Particles, *Jour. of Coll. & Interface Sci.*, 301:155-167.

Cai, J., and Sorensen, C.M. (1994). Diffusion of Fractal Aggregates in the Free Molecular Regime, *Phys. Rev. E* 50:3397-3400.

Cai, J., Lu, N., and Sorensen, C.M. (1995). Analysis of Fractal Cluster Morphology Parameters: Structural Coefficient and Density Autocorrelation Function Cutoff, *J. Coll. Int. Sci.* 171:470-474.

Chan, P., and Dahneke, B. (1981). Free-Molecule Drag on Straight Chains of Uniform Spheres, *J. Appl. Phys.* 52:3106-3110.

Chen, Z.Y., Meakin, P., and Deutch, J.M. (1987). Comment on "Hydrodynamic Behavior of Fractal Aggregates, *Phys. Rev. Lett*. 59:2121.

Cheng, Y.-S., Allen, M. D., Gallegos, D. P., Yeh, H.-C., and Peterson, K. (1988).Drag Force and Slip Correction of Aggregate Aerosols, *Aerosol Sci. Technol.* 8: 199-214.

Cho, K., Hogan Jr., C.J. and Biswas, P. (2007). Study of the Mobility, Surface Area, and Sintering Behavior of Agglomerates in the Transition Regime by Tandem Differential Mobility Analysis, *J. Nanopart. Res.* 9:1003-1012.

Dahneke, B. (1982). Viscous Resistance of Straight-Chain Aggregates of Uniform Spheres, *Aerosol Sci. Tech.* 1:179-185.

DeCarlo, P.F., Slowik, J.G., Worsnop, D.R., Davidovits, P., and Jimenez, J.L. (2004). Particle Morphology and Density Characterization by Combined Mobility ad Aerodynamic Diameter Measurements. Part 1: Theory, *Aerosol Sci. Technol*. 38:1185-1205.

Filippov, A.V. (2000). Drag and Torque on Clusters of N Arbitrary Spheres at Low Reynolds Number, *Jour. of Coll. & Inteface Sci*., 229:184-195.

Friedlander, S. K. (2000). *Smoke, Dust and Haze. Fundamentals of Aerosol Dynamics.* Oxford University Press, New York.

Gwaze, P., Schmid, O., Annegarn, H.J., Andreae, M.O., Huth, J., and Helas Günter (2006). Comparison of Three Methods of fractal Analysis Applied to Soot Aggregates from Wood Combustion, *J. Aerosol Sci.* 37:820-838.

Horvath H. (1974). The sedimentation behavior of non-spherical particles, *Staub* 34: 197-202.

Jullien, R. and Botet, R. (1987). *Aggregation and Fractal Aggregates*, World Scientific, Singapore.

Katzel, U., Bedrich, R., Stintz, M., Ketzmerick, R., Gottschalk-Gaudig, T., and Barthel, H., (2008). *Part. Part. Syst. Charact.* 25: 9-18.

Kasper, G., Niida, T., and Yang, M. (1985). *J. Aerosol Sci.* 16:535-556.

Kim, W. G., Sorensen, C.M., Chakrabarti, A. (2004). Universal Occurrence of Soot Aggregates with a Fractal Dimension of 2.6 in Heavily Sooting Laminar Diffusion Flames, *Langmuir* 20:3969-3973.

Kim, W.G., Sorensen, C.M., Fry, D. and Chakrabarti, A. (2006). Soot Aggregates, Superaggregates and Gel-Like Networks in Laminar Diffusion Flames, *J. Aerosol Sci.* 37:386-401.

Kirkwood, J.G., and Riseman, J. (1948). The Intrinsic viscosities and Diffusion Constants of Flexible Macromolecules in Solution, *J. Chem. Phys.* 16:565-573.

Kolb, M., Botet, R., and Jullien, R. (1983). Scaling of Kinetically Growing Clusters, *Phys. Rev. Lett.* 51:1123-1126.

Kousaka, Y., Endo, Y., Ichitsubo, H. and Alonso, M., (1996). Orientration-Specific Dynamic Shape Factors for Doublets and Triplets of Spheres in the Transition Regime, *Aerosol Sci. Technol.* 24:36-44.

Koylu, U.O. and Faeth, G.M. (1995). Optical Properties of Overfire Soot in Buoyant Turbulent Diffusion Flames at Long Residence Times. *Trans. of ASME* 116:152-159.

Lattuada, M., Wu, H., and Morbidelli, M. (2003a). Hydrodynamic Radius of Fractal Clusters, *Jour. of Coll. & Interface Sci.* 268:96-105.

Lattuada, M., Wu, H., and Morbidelli, M. (2003b). A Simple Model for the Structure of Fractal Aggregates, *Jour. Coll. and Interface Sci.* 268:106-120.

Mackowski, D.W. (2006). Monte Carlo Simulation of Hydrodynamic Drag and Thermophoresis of Fractal Aggregates of Spheres in the Free-Molecular Flow Regime, *J. Aerosol Sci.* 37:242-259.

Maricq, M.M., and Xu, N. (2004). The Effective Density and Fractal Dimension of Soot Particles from Premixed Flames and Motor Vehicle Exhaust, *J. Aerosol Sci.* 35:1251-1274.

Meakin, P. (1983). Formation of Fractal Clusters and Networks by Irreversible Diffusion Limited Aggregation, *Phys. Rev. Lett.* 51:1119-1122.

Meakin, P., Fractal Aggregates (1988). *Adv. Coll. & Interface Sci.* 28:249-331.

Meakin, P., Chen, Z.Y., and Deutch, J.M. (1985). The Translational Friction Coefficient and Time Dependent Cluster Size Distribution of Three Dimensional Cluster-Cluster Aggregation, *J. Chem. Phys.* 82:3786-3787.

Meakin, P., Donn, B. and Mulholland, G. W. (1989). Collisions between point mass and fractal aggregates, *Langmuir,* 5:510-518.

Mountain, R. D. and Mulholland, G. W. (1988). Light-scattering from simulated smoke agglomerates, *Langmuir* 4:1321-1326.

Park, K., Kittelson, D.B., and McMurry, P.H. (2004). Structural Properties of Diesel Exhaust Particles Measured by Transmission Electron Microscopy (TEM): Relationships to Particle Mass and Mobility, *Aerosol Sci. Technol.* 38:881-889.

Pierce, F., Sorensen, C.M., and Chakrabarti, A. (2006). Computer Simulation of Diffusion-Limited Cluster-Cluster Aggregation with an Epstein Drag Force, *Phys. Rev. E* 74:021411-8.

Pusey, P. N., Rarity, J. G., Klein, R., Weitz, D. A. (1987). Comment on "Hydrodynamic behaviour of fractal aggregates", *Phys. Rev. Lett*. 59:2122-2125.

Rogak, S. N., Flagan, R. C. and Nguyen, H. V. (1993). The mobility and structure of aerosol agglomerates, *Aerosol Sci. Technol*. 18:25-47.

Rogak, S. N. and Flagan, R. C. (1990). Stokes drag on self-similar structures of spheres, *J. Coll. Int. Sci.* 134:206-218.

Schmidt-Ott, A. (1988). In Situ Measurement of the Fractal Dimensionality of Ultrafine Aerosol Particles, *Appl. Phys. Lett*. 52:954-956.

Shin, W.G., Mulholland, G.W., Kim, S.C., Wang, J., Emery, M.S. and Pui, D.Y.H. (2009). Friction Coefficient and Mass of Silver Agglomerates in the Transition Regime, *J. Aerosol Science* 40:573-587.

Shin, W.G., Mulholland, and Pui, D.Y.H. (2010). Determination of Volume, Scaling Exponents, and Particle Alignment of Nanoparticle Agglomerates using Tandem Differential Mobility Analyzers, *J. Aerosol Science* 41:665-681.

Slowik, J.G., Stainken, K., Davidovits, P., Williams, L.R., Jayne, J.T., Kolb, C.E., Worsnop, D.R., Rudich, Y., DeCarlo, P.F., and Jimenez, J.L. (2004). Particle Morphology and Density Characterization by Combined Mobility and Aerodynamic Diameter Measurements. Part 2: Application to Combustion-Generated Soot Aerosols as a Function of Fuel Equivalence Ratio, *Aerosol Sci. Technol.* 38:1206-1222.

Sorensen, C. M. (2001). Light Scattering from Fractal Aggregates. A Review, *Aerosol Sci. Technol.* 35:648-687.

Sorensen, C. M., Cai, J. and Lu, N. (1992). Light Scattering Measurements of Monomer Size, Monomers per Aggregate and Fractal Dimension for Soot Aggregates in Flames, *Appl. Optics* 31, 6547-6556.

Sorensen, C.M., and Roberts, G.C. (1997). The Prefactor of Fractal Aggregates, *Jour. of Coll. & Interface Sci.*, 186:447-452.

Sorensen, C. M. and Oh, C. (1998). Divine Proportion Shape Invariance and the Fractal Nature of Aggregates, *Phys. Rev.* E58:7545-7548.

Sorensen, C.M. and Wang, G.M. (1999). Size Distribution Effect on the Power Law Regime of the Structure Factor of Fractal Aggregates, *Phys. Rev.* E60:7143-7148.

Sorensen, C.M., and Wang, G.M. (2000). Note on the Correction for Diffusion and Drag in the Slip Regime, *Aerosol Sci. Technol.* 33:353-356.

Sorensen, C. M., W. Kim, D. Fry, and A. Chakrabarti (2003). Observation of Soot Superaggregates with a Fractal Dimension of 2.6 in Laminar Acetylene/Air Diffusion Flames, *Langmuir* 19:7560-7563 (2003).

Tandon, P. and Rosner, D. E. (1995). Translational Brownian diffusion-coefficient of large (multiparticle) suspended aggregates, *Ind. Eng. Chem. Res.* 34:3265-3277.

Van Gulijk, C., Marijnissen, J.C.M., Makkee, M., Moulijn, J.A., and Schmidt-Ott, A. (2004). Measuring Diesel Soot with a Scanning Mobility Particle Sizer and an Electrical Low-Pressure Impactor: Performance Assessment with a Model for Fractal-Like Agglomerates, *J. Aerosol Sci.* 35:633-655.

Wang, G.M. and Sorensen, C.M. (1999).Diffusive Mobility of Fractal Aggregates over the Entire Knudsen Number Range, *Phys. Rev.* E60:3036-3044

Wiltzius, P. (1987). Hydrodynamic behavior of fractal aggregates, *Phys. Rev. Lett.* 58:710-713.

Zelenyuk, A., Cai, Y., and Imre, D. (2006). From Agglomerates of Spheres to Irregularly Shaped Particles: Determination of Dynamic Shape Factors from Measurements of Mobility and Vacuum Aerodynamic Diameters, *Aerosol Sci. Technol.* 40:197-217.